

Investigation of the effects of gas-counter-pressure injection molding on the properties and manufacturability of post-consumer recycled polypropylene

BORTOLETTO Anna^{1,a*}, BOVO Enrico^{1,b}, SORGATO Marco^{1,c} and LUCCHETTA Giovanni^{1,d}

¹Department of Industrial Engineering, University of Padova, Via Venezia 1, 35131, Padova, Italy

^aanna.bortoletto.4@phd.unipd.it, ^benrico.bovo.1@phd.unipd.it, ^cmarco.sorgato@unipd.it, ^dgiovanni.lucchetta@unipd.it

Keywords: Gas Counter Pressure, Injection Molding, Recycling, Post-Consumer Polypropylene

Abstract. In contemporary times, the most effective strategy for mitigating the environmental effects of plastics and their manufacturing is recycling. However, producing high-quality items from recycled materials remains a challenge. This study addresses these challenges, specifically focusing on the injection molding process for recycled polypropylene. Key issues identified include poor surface finish of the molded items, mold contamination with oily residues, and strong odors during processing. The proposed solution involves the innovative use of gas counter pressure in conjunction with injection molding. The study explores various nitrogen pressure levels to assess their impact. Findings indicate that an optimal pressure level significantly improves the surface quality of the products and reduces the accumulation of dirt in the mold cavities. While gas counter pressure does not mitigate odor emissions, it represents a promising step forward in developing a high-quality recycled polypropylene compound. This approach could pave the way for more advanced recycling techniques, enhancing the quality of products made from recycled plastics.

Introduction

Plastic demand has increased exponentially over the last few decades, pushing the production from 1.5 million tons in 1950 to more than 390 million tons in 2021 [1 - 2]. Recycling is considered the best solution to reduce plastic's environmental impact because it decreases the need for virgin material in the production of new components and the quantity of underground waste [3 - 4].

There are two different categories of plastic that can be recycled, distinguished by their source. The first is post-industrial (PIR) waste, which comes directly from the industry (scrap material, non-conforming pieces, feeding systems, etc). The second category is post-consumer (PCR) waste, which derives from the urban collection of waste: different types of materials and plastics are mixed, and they are contaminated, for example, by organic residues of food or dirt [5 - 6]. Recycling PCR waste is still an open challenge that requires improvement in each processing step to produce a high-quality material and product.

Within post-consumer waste, one of the most interesting plastics to study is recycled polypropylene (PP), the primary material used in Europe's plastic-intensive packaging industry [7]. Polypropylene also exhibits characteristics that make it potentially suitable for upcycling, with the right combination of mechanical recycling, compounding, and injection molding parameters. Upcycling consists of using recycled materials to manufacture a product with greater value than the previous one [8]. Currently, upcycling faces limitations caused due to issues arising during the re-processing of rPP through injection molding [9]. The origin of these issues can be traced to

contaminating absorbed during the first usage of PP, because of the material's high permeability. These contaminants, which may include organic residues from food, inks, adhesives, or others [10 - 11], remain in the rPP even after the cleaning steps of the recycling process. When exposed to the high temperatures and shear stresses of the injection molding, they undergo degradation, affecting the manufacturability of the material. Specifically, issues such as a compromised surface appearance, odorous emissions, and contamination of the mold cavity surface with oily substances can be observed [12]. These problems will be analyzed one by one in the following paragraphs.

The surface of parts molded using PCR PP is often altered by white/light-grey stripes elongated along the flow direction [13], commonly referred as silver streaks. Degraded contaminants within the plastic melt form gas bubbles that expand when they reach the flow front, as they are subjected to a pressure close to the atmospheric conditions. The bubbles are then pushed by the fountain flow to the walls of the cavity [14], where they break and freeze within the skin layer forming silver streaks. In MicroCellular Injection Molding, the use of high mold temperature increases the surface quality [15]. A hot mold allows the skin layer to keep a certain fluidity, and the flowing heart's material pushes the base of the bubbles little by little until closure. In recent studies, the technology of gas counter pressure was applied to MuCell to solve the silver streaks problem [16 - 17]. Gas counter pressure consists of injecting pressurized gas, usually nitrogen or carbon dioxide, from the opposite direction of the polymer melt to counteract the expansion of the degraded gases [18].

The presence of silver streaks on the part's surface not only represents an aesthetic problem but also causes the accumulation of dirt on the mold cavity surface. Gases condense on colder cavity walls, releasing oily and greasy components that clog the vents and accumulate in the mold cavity, forming a film of dirt. Sorgato et al. proposed a self-cleaning solution to mold vent clogging by exploiting laser-induced surface structures [19].

Some of the degraded gases emit a strong odor that is partially released in the environment immediately after production and partially throughout the components' life. Van Laere et al. found 203 VOCs (volatile organic compounds) in plastic waste from the food packaging industry and 142 VOCs in other packaging products [20]. Addressing the strong odor of recycled plastic is crucial for its indoor applications, where it is necessary to grant safety and comfort for the users. Different tests were conducted by Prado et al. to verify if recycled PCR PP filled with talc could conform to the emissions norms of automotive. The results showed that the components were above the acceptance limits for all three different tests: GMW 3205, VDA 270, and ISO 13299 [21]. Fraunhofer ICT adopted the extrusion process with a stripping agent to reduce the plastic's aroma. The stripping was performed using a supercritical fluid (carbon dioxide) to remove odorous substances from the melt in a twin-screw co-rotating extruder [22 - 23]. Water or nitrogen were also used as stripping agents [24].

Given the various challenges identified in the literature, there is a clear need for innovative solutions, particularly regarding the issue of mold contamination and odorous emissions in PCR PP. This gap in the current research landscape sets the stage for our investigation. Thus, through the contributions of previous studies, this research aims to test a new application of the GCP technique to address these specific challenges in molding PCR PP. Different gas counter-pressure levels were used, and their effect was compared to the outcome of the traditional injection molding process. The influence of the pressure on the defects and the mold contamination was analyzed through image analysis, while a fogging test was used to determine its effect on odor emissions.

Materials and methods

Injection Molding. The injection molding experiments were conducted using a 100% recycled Polypropylene (rPP) from Sirmax S.p.a. called Sertene X200C RC. It is a non-filled polypropylene, recycled from post-consumer waste, mainly food packaging.

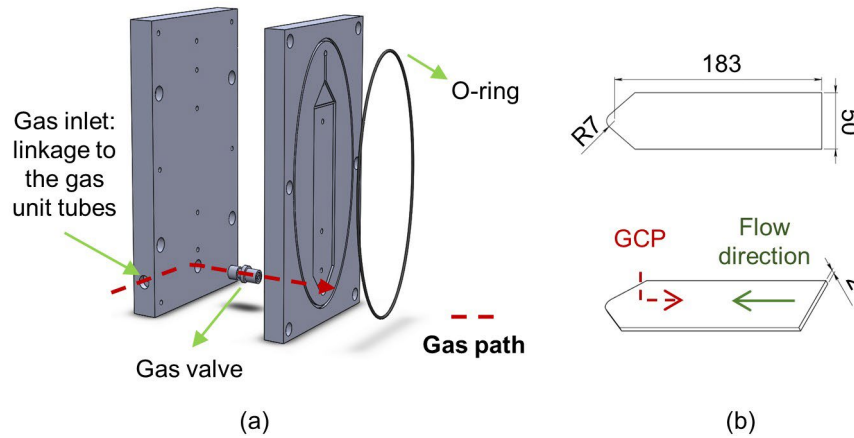


Fig. 1 - Prototypal mold suitable for GCP usage (a); specimen to perform the analysis (b).

The specimen is a plate with dimensions of 183 mm x 50 mm x 2 mm (Fig. 1b), molded with a full-hydraulic Battenfeld HM 110/525H/210s. The injection molding machine is linked to the gas counter pressure system, which consists of compressor control module by Maximator (RM/500/2/VP/80/500/N2). It works through a pneumatic compressor that takes the nitrogen from a tank at 180 bar and compresses it to the desired pressure. The gas path to reach the cavity is displayed in Fig. 1a. Nitrogen enters the cavity through a gas valve placed at the opposite side from the gate and an O-ring was placed around the cavity to avoid any leakage. (Fig. 1a). The signal to start the injection of the gas is given by a sensor that is activated at the closure of the two plates of the mold with a limit switch.

The injection molding parameters used for defects and mold contamination analysis are displayed in Table 2. The only variable is the gas level of GCP, as it is the primary focus of this work.

Table 1. Injection molding parameters to mold the specimens for the analysis.

Parameter	Value
Melt temperature (T_{melt})	250 °C
Mold temperature (T_{mold})	40 °C
Residence time (t_{res})	120 s
GCP holding time	2 s
Gas pressure (GCP)	0; 15; 40; 60 bar

For the analysis of the emissions, only the extreme values of gas counter pressure were tested (0 bar and 60 bar). A more thorough testing campaign was not carried out on this matter because the initial results showed a complete lack of improvements, as it will be seen in the specific section.

Superficial Defects Evaluation. A method based on image analysis was used to evaluate the defects on the molded plate surface. This was possible thanks to the color difference between the defect and the clean base material. Photos were taken using a repeatable setting with the professional camera Nikon D3500. Twenty plates were analyzed for each nitrogen level to have a statistical sample variation and the analysis was conducted using the programming language of Python. From the raw photo, some processing was made to gradually reduce the area to study to

the region between the two ejectors, eliminating the background (Fig. 2a). This region was called ROI and transformed into grayscale before the defects evaluation.

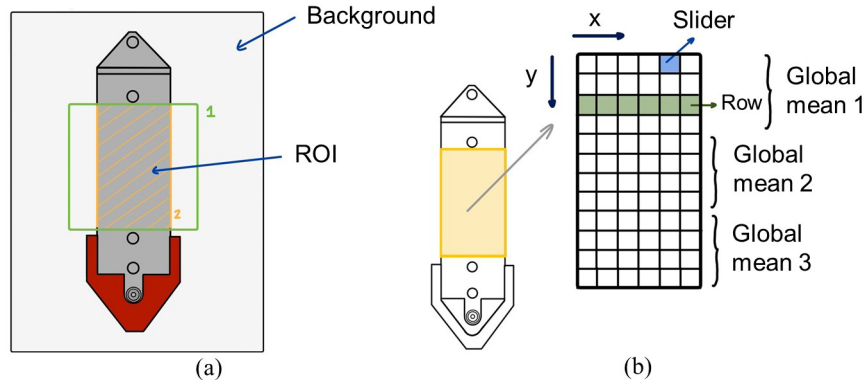


Fig. 2 – Definition of the region of interest (a); explanation of the strategy used by the code to evaluate the standard deviation (b).

The ROI was divided into a grid of 6000 rectangles (20 columns, 300 rows). These rectangles were called sliders, and for each of them, the value of the standard deviation of the plate color was calculated and then averaged with the values of the same row (Fig. 2b).

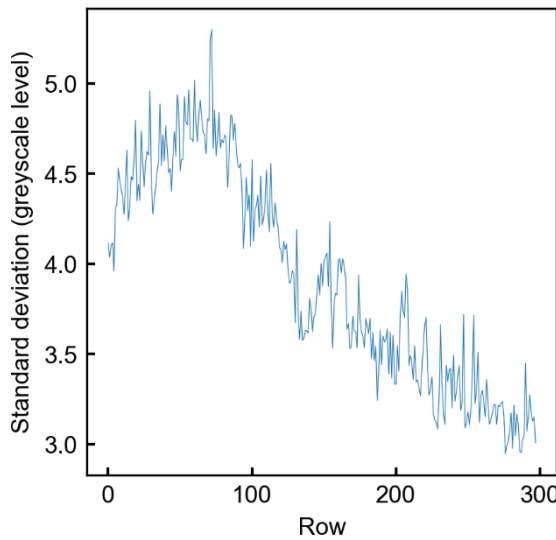


Fig. 3 - Output of the Python code: graph with the 300 values of standard deviation for each row.

The code output was one value of standard deviation per row, from 1 to 300, displayed in a graph similar to the one in Fig. 3. The higher the standard deviation is, the more different the color of the molded piece is from the clean material.

Mold Contamination Evaluation. Photos of the mold were taken and then processed with a Python code to evaluate the dirt accumulated on the cavity surface. This strategy worked once again thanks to a difference of color, between the clean and dirt areas of the mold cavity surface. The cavity surface was photographed after molding 50 plates for each set of parameters with a repetitive setup. The image analysis was conducted using Python. Before the quantification of the accumulated dirt, photos were processed in the following way:

- the region of interest was reduced to an area between the holes for the ejectors, leaving the borders out of the selection;

- the resulting image was transformed into a grayscale.

The analysis was based on an Otsu thresholding [25], which means that the image was transformed into a binary mode with only two levels of color (black and white). The white is identified with level 255, while the black has level 0. Each pixel is assigned to black or white based on its grey value compared to the threshold one: if it is higher than the threshold, it becomes white; if it is lower, it becomes black.

Emissions Evaluation. Following DIN 75201, the fogging test was used to evaluate emissions. This test quantifies volatile compounds (VOCs) emitted from a specimen under specified conditions, but it cannot identify them. Thus, the results do not indicate how much of the calculated emissions are odorous, but they highlight a possible improvement in the general emission of VOCs thanks to the use of GCP. The required equipment includes a fogging machine, cooling device, beakers, glass plates, metal and fluorocarbon rubber rings, aluminum foils (103 mm diameter, 0.03 mm thickness), and an analytical balance with a 0.01 mg accuracy. Thermofisher's Horizon FTS (Fog Testing System) with a recirculating chiller Accel 250LC was used.

The specimens were cut to have a circular shape with a diameter of (80 ± 1) mm, and two disks were stuck inside the beaker to reach the weight of (10 ± 2) g. The beaker was closed with one sealing ring, one aluminum foil, one glass plate, and one cooling plate. The aluminum foil was weighed before the test with an accuracy of ± 0.01 mg. The beaker was left inside the machine for $16 \text{ hours} \pm 10 \text{ minutes}$ at a temperature of 100 ± 0.5 °C, after which the aluminum foil was dried in a desiccator with silica gel for 4 hours. The output was the difference in weight of the foil from before to after the test, which identifies the amount of condensable components in the specimen. The test was repeated six times for each set of GCP parameters.

Results and discussion

Superficial Defects. For each value of gas counter pressure, 20 plates were photographed and analyzed, and the code's output was a graph with 300 values of standard deviation along the region of interest. From these outputs, a mean graph was created, as depicted in Fig. 4, where the values of global means are also reported in the areas they correspond to.

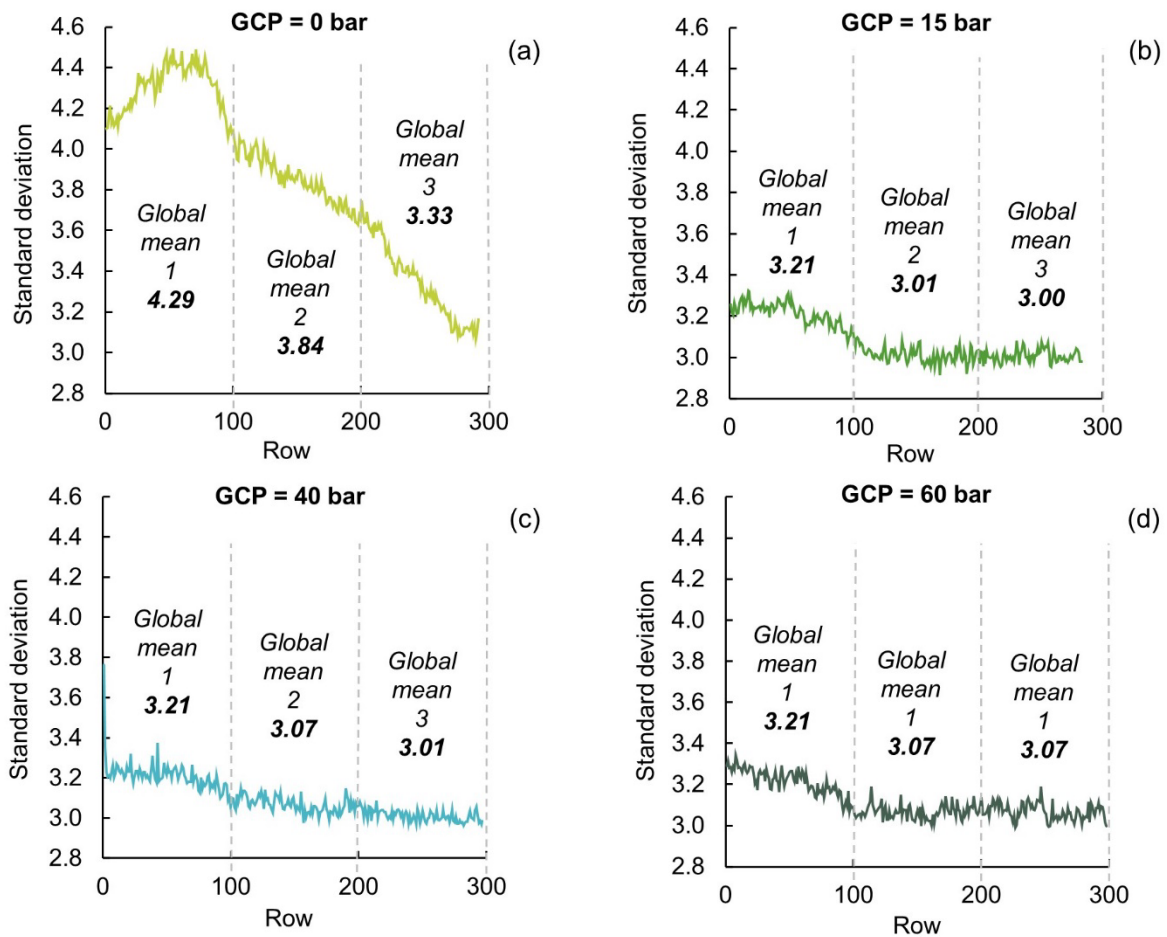


Fig. 4 - Results of defects evaluation in terms of standard deviation. (a) GCP = 0 bar; (b) GCP = 15 bar; (c) GCP = 40 bar; (d) GCP = 60 bar. The global means are displayed in the corresponded areas.

For the standard injection molding (GCP = 0 bar), the standard deviation computed as global mean 1 is equal to 4.29 in the region near the gate. This value rapidly decreases towards the end of the cavity, reaching its minimum at 3.33. The slope of the curve is high, indicating a heterogeneous specimen in terms of color and, therefore, defects along its length. The defects are not distributed equally but are gathered in the first region after the gate and then fade towards a global mean 2 of 3.84 and a global mean 3 of 3.33. For the plates molded with gas pressure (15, 40, and 60 bar), the curve's trend is flatter, as they start from a lower value (3.21) and finish at around 3.00. This means that the defects are less present, and there is no great difference between the region near the gate and the end of the specimen.

The values of global mean 3 between the sets with GCP and the set with no GCP are almost comparable, and this result is representative of what can be seen in the plates, where the furthest region from the gate is clean from defects. The area near the gate is where the most silver streaks emerge because, when the bubbles created by the degraded contaminating substances reach the cavity, they expand for the lower pressure. The fountain flow then pushes them toward the walls, where they explode and form the defect. Gas counter pressure has a positive effect on the superficial appearance of the specimens because it communicates an opposite pressure to the flow front and makes the bubbles implode and close before they can reach the surface of the product.

From Fig. 4 it is also possible to notice that the results remain unvaried regarding standard deviation increasing the pressure level from 15 to 40 to 60 bar. Therefore, there is no need to use

high nitrogen levels to reach good results for the surface appearance. From an economic point of view, it is preferable to use the lowest possible values.

Mold Contamination. For each set of parameters, Fig. 5 reports the grayscale cut image, the thresholded image, and a pie chart with the percentage of white pixels (indicating the dirt) in comparison to the black ones (indicating the clean mold surface).

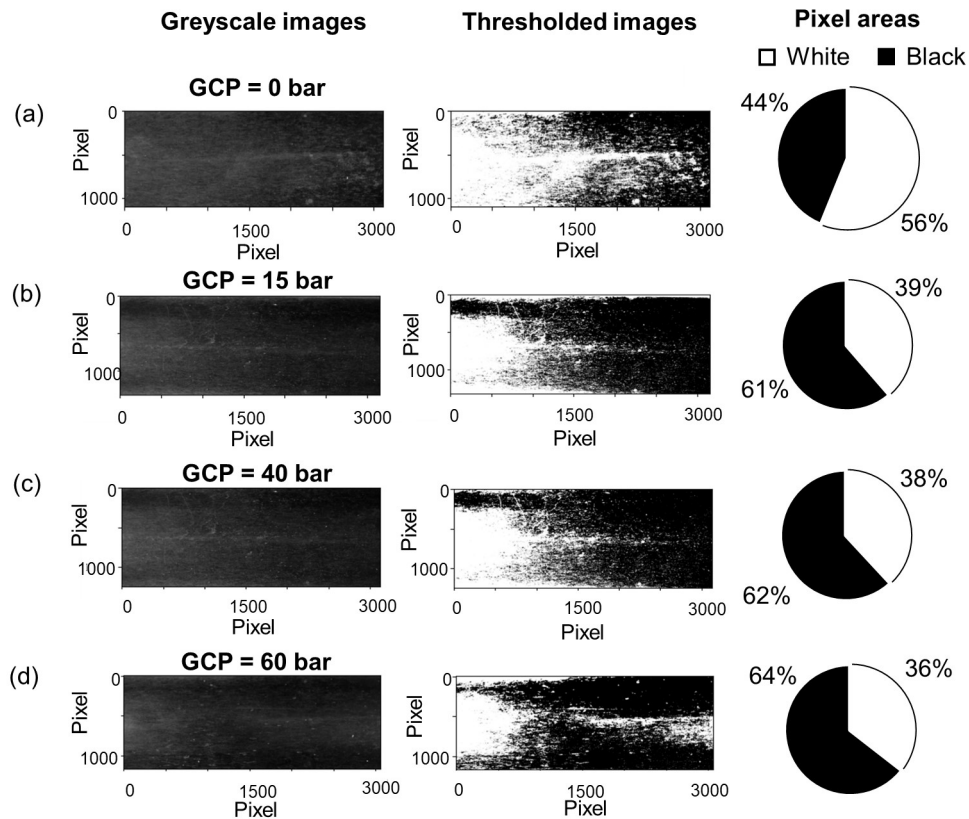


Fig. 5 - Results of mold contamination. The pie charts indicate the area occupied by the dirt in the image (white pixels). (a) GCP = 0 bar, (b) GCP = 15 bar, (c) GCP = 40 bar, (d) GCP = 60 bar.

After molding 50 plates with a no GCP injection molding process, the dirt accumulated on the cavity surface could be seen with the naked eye and corresponded to an area of 56% of the analyzed images. It presented itself with the same shape and distribution of the silver streaks on the specimen: elongated along the flow direction, more intense near the gate, and slowly fading. Therefore, the dirt appears on the cavity surface where the bubbles of contaminants explode; the fewer silver streaks on the surface of the specimens, the cleaner the mold will be. In this particular case, the streaks of dirt had an orange nuance. Using gas counter pressure at 15 bar there was a significant 17 % difference from the previous case: the dirty area was less expanded and it had a grey/white color. The results with 40 and 60 bar showed a slight improvement of a few percentage points, as can be seen by the images and the graphs (Fig. 5).

The results show that using gas counter pressure, the accumulation of dirt on the mold cavity surface decreases significantly by around 17%. Therefore, gas counter pressure can solve both the superficial defects and the mold contamination simultaneously, with a proportional effect between the two. The difference between 15, 40, and 60 bar is minimal (1-2%), which is congruent to the

effect of GCP on the silver streaks, where the global mean 1 of the different nitrogen levels was the same (3.21).

It is important to report that even after cleaning the mold cavity surface with an acetone-based solvent, a ring of dirt remained on it. This ring affected the results from Python, which included it in the white pixels areas, even if it was not dirty and oily. The improvement of the cleanliness of the cavity surface could potentially be higher than the 15/20 % obtained from these results.

Emissions. The output is the difference in the weight of the aluminum foil between after and before the test. The test was repeated six times for each set of parameters, and a mean value was calculated from the six output values. The two means are displayed in Fig. 6 with their standard deviation, which represents the error of the test.

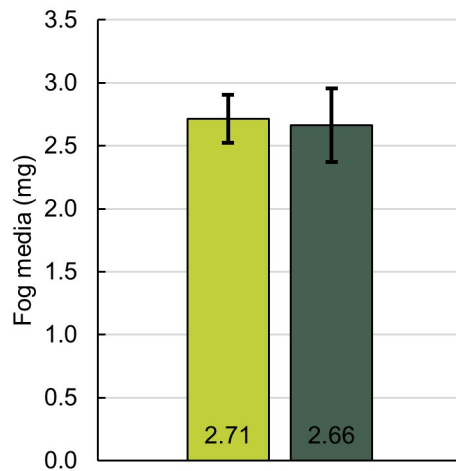


Fig. 6 - Results of fogging test. The error band is the standard deviation of the values of the six tests.

What can be observed from this graph is that the use of the gas counter pressure has no benefit on the plastic odor, as the weight of the aluminum foil varies from 2.71 mg to 2.66 mg, but the error bands overlap. It is reasonable to say that gas counter pressure may be able stop the contaminating substances from emerging to the surface and limit their manifestation as silver streaks or dirt. However, the odorous compounds remain in the heart of the specimen. Even if the contaminating volatile substances are enclosed inside the product, they can reach the environment and disperse in it because of the high permeability of the polypropylene.

Conclusions

In this work, a new application of gas counter pressure was investigated with the aim of obtaining high-quality injection molded products with recycled polypropylene. The experiments showed that gas counter pressure using nitrogen can:

- eliminate silver streaks from a visual point of view and decrease the color non-uniformity of 21% in the gate area, computed as standard deviation with image analysis;
- decrease mold contamination by around 20% when analyzed through image thresholding.

On the other hand, the emissions of volatile substances (VOCs) inside the plastic could not be reduced using GCP: the results of the fogging test showed the same quantity of emissions for the parameters studied.

To summarize, results suggest that employing a relatively low GCP value near the established threshold is advisable for the following reasons:

- the reduced usage of nitrogen makes the technology more cost-effective and more suitable for a possible scale-up in a real production line;

- on the specimens' surface, no discernible difference could be found between low- or high-pressure values.

These results can be a starting point to improve the processability of rPP and to obtain a high-quality product that can be used for aesthetic applications. Further studies need to be conducted to solve the problem regarding odor emissions, which could open many industrial sectors to using recycled plastics.

References

- [1] European Parliament, Plastic Waste and Recycling in the EU: numbers and figures, 2018.
- [2] Plastics Europe and EPRO, Plastics - the Facts 2022, 2022.
- [3] J. Hopewell, R. Dvorak, and E. Kosior, Plastics recycling: Challenges and opportunities, *Philosophical Transactions of the Royal Society B: Biological Sciences*, vol. 364, no. 1526. Royal Society, pp. 2115–2126, Jul. 27, 2009. <https://doi.org/10.1098/rstb.2008.0311>
- [4] M. K. Eriksen, A. Damgaard, A. Boldrin, and T. F. Astrup, Quality Assessment and Circularity Potential of Recovery Systems for Household Plastic Waste, *J Ind Ecol*, vol. 23, no. 1, pp. 156–168, Feb. 2019. <https://doi.org/10.1111/jiec.12822>
- [5] K. Ragaert, L. Delva, and K. Van Geem, Mechanical and chemical recycling of solid plastic waste, *Waste Management*, vol. 69. Elsevier Ltd, pp. 24–58, Nov. 01, 2017. <https://doi.org/10.1016/j.wasman.2017.07.044>
- [6] A. Schulte, B. Kampmann, and C. Galafton, Measuring the Circularity and Impact Reduction Potential of Post-Industrial and Post-Consumer Recycled Plastics, *Sustainability*, vol. 15, no. 16, p. 12242, Aug. 2023. <https://doi.org/10.3390/su151612242>
- [7] H. Dahlbo, V. Poliakova, V. Mylläri, O. Sahimaa, and R. Anderson, Recycling potential of post-consumer plastic packaging waste in Finland, *Waste Management*, vol. 71, pp. 52–61, Jan. 2018. <https://doi.org/10.1016/j.wasman.2017.10.033>
- [8] X. Zhao et al., Plastic waste upcycling toward a circular economy, *Chemical Engineering Journal*, vol. 428. Elsevier B.V., Jan. 15, 2022. doi: 10.1016/j.cej.2021.131928.
- [9] Z. O. G. Schyns and M. P. Shaver, Mechanical Recycling of Packaging Plastics: A Review, *Macromolecular Rapid Communications*, vol. 42, no. 3. Wiley-VCH Verlag, Feb. 01, 2021. <https://doi.org/10.1002/marc.202000415>
- [10] A. K. Undas, M. Groenen, R. J. B. Peters, and S. P. J. van Leeuwen, Safety of recycled plastics and textiles: Review on the detection, identification and safety assessment of contaminants, *Chemosphere*, vol. 312, Jan. 2023. <https://doi.org/10.1016/j.chemosphere.2022.137175>
- [11] W. Camacho and S. Karlsson, Quality-determination of recycled plastic packaging waste by identification of contaminants by GC–MS after microwave assisted extraction (MAE), *Polym Degrad Stab*, vol. 71, no. 1, pp. 123–134, Jan. 2000. [https://doi.org/10.1016/S0141-3910\(00\)00163-4](https://doi.org/10.1016/S0141-3910(00)00163-4)
- [12] X. Zhao, B. Boruah, K. F. Chin, M. Đokić, J. M. Modak, and H. Sen Soo, Upcycling to Sustainably Reuse Plastics, *Advanced Materials*, vol. 34, no. 25. John Wiley and Sons Inc, Jun. 01, 2022. <https://doi.org/10.1002/adma.202100843>
- [13] J. Hou, G. Zhao, G. Wang, G. Dong, and J. Xu, A novel gas-assisted microcellular injection molding method for preparing lightweight foams with superior surface appearance and enhanced mechanical performance, *Mater Des*, vol. 127, pp. 115–125, Aug. 2017. <https://doi.org/10.1016/j.matdes.2017.04.073>

- [14] H. Yokoi, N. Masuda, and H. Mitsuhashi, Visualization analysis of flow front behavior during filling process of injection mold cavity by two-axis tracking system, *J Mater Process Technol*, vol. 130–131, pp. 328–333, Dec. 2002. [https://doi.org/10.1016/S0924-0136\(02\)00742-2](https://doi.org/10.1016/S0924-0136(02)00742-2)
- [15] S. C. Chen, Y. W. Lin, R. Der Chien, and H. M. Li, Variable mold temperature to improve surface quality of microcellular injection molded parts using induction heating technology, in *Advances in Polymer Technology*, 2008, pp. 224–232. <https://doi.org/10.1002/adv.20133>
- [16] J. Ren, L. Lin, J. Jiang, Q. Li, and S. S. Hwang, Effect of Gas Counter Pressure on the Surface Roughness, Morphology, and Tensile Strength between Microcellular and Conventional Injection-Molded PP Parts, *Polymers (Basel)*, vol. 14, no. 6, Mar. 2022. <https://doi.org/10.3390/polym14061078>
- [17] S. C. Chen, P. S. Hsu, and S. S. Hwang, The effects of gas counter pressure and mold temperature variation on the surface quality and morphology of the microcellular polystyrene foams, *J Appl Polym Sci*, vol. 127, no. 6, pp. 4769–4776, Mar. 2013. <https://doi.org/10.1002/app.37994>
- [18] F. A. Shutov, *Integral/Structural Polymer Foams*. Springer Berlin Heidelberg, 1986. <https://doi.org/10.1007/978-3-662-02486-7>
- [19] M. Sorgato, F. Zanini, D. Masato, and G. Lucchetta, Submicron laser-textured vents for self-cleaning injection molds, *J Appl Polym Sci*, vol. 137, no. 42, Nov. 2020. <https://doi.org/10.1002/app.49280>
- [20] M. Roosen et al., Tracing the origin of VOCs in post-consumer plastic film bales, *Chemosphere*, vol. 324, May 2023. <https://doi.org/10.1016/j.chemosphere.2023.138281>
- [21] K. S. Prado et al., Odor characterization of post-consumer and recycled automotive polypropylene by different sensory evaluation methods and instrumental analysis, *Waste Management*, vol. 115, pp. 36–46, Sep. 2020. <https://doi.org/10.1016/j.wasman.2020.07.021>
- [22] I. Mikonsaari, E. van de Walle, and K. Moser, Physical Recycling of Plastics - Providing Recyclates with Reduced Emissions, *Kunststoffe international*, vol. 8, 2022, Accessed: Oct. 16, 2023. [Online]. Available: <https://publica.fraunhofer.de/handle/publica/430119>
- [23] Fraunhofer, Extractive extrusion process performed with all provided material classes, 2021. Available: www.creatorproject.eu
- [24] A. Cabanes, F. J. Valdés, and A. Fullana, A review on VOCs from recycled plastics, *Sustainable Materials and Technologies*, vol. 25. Elsevier B.V., Sep. 01, 2020. <https://doi.org/10.1016/j.susmat.2020.e00179>
- [25] N. Otsu, “A Threshold Selection Method from Gray-Level Histograms,” *IEEE Transactions on Systems, Man, and Cybernetics*, vol. 9, no. 1, pp. 62–66, Jan. 1979. <https://doi.org/10.1109/TSMC.1979.4310076>